A high-field solid-state $^{35/37}$Cl NMR and quantum chemical investigation of the chlorine quadrupolar and chemical shift tensors in amino acid hydrochlorides†

Rebecca P. Chapman and David L. Bryce*

Received 17th August 2007, Accepted 17th October 2007
First published as an Advance Article on the web 8th November 2007
DOI: 10.1039/b712688c

A series of six L-amino acid hydrochloride salts has been studied by $^{35/37}$Cl solid-state NMR spectroscopy (at 11.75 and 21.1 T) and complementary quantum chemical calculations. Analyses of NMR spectra acquired under static and magic-angle-spinning conditions for the six hydrochloride salts, those of aspartic acid, alanine, cysteine, histidine, methionine and threonine, allowed the extraction of information regarding the chlorine electric field gradient (EFG) and chemical shift tensors, including their relative orientation. Both tensors are found to be highly dependent on the local environment, with chlorine-35 quadrupolar coupling constants (C_Q) ranging from −7.1 to 4.41 MHz and chemical shift tensor spans ranging from 60 to 100 ppm; the value of C_Q for aspartic acid hydrochloride is the largest in magnitude observed to date for an organic hydrochloride salt. Quantum chemical calculations performed on cluster models of the chloride ion environment demonstrated agreement between experiment and theory, reproducing C_Q to within 18%. In addition, the accuracy of the calculated values of the NMR parameters as a function of the quality of the input structure was explored. Selected X-ray structures were determined (L-Asp HCl; L-Thr HCl) or re-determined (L-Cys HCl · H_2O) to demonstrate the benefits of having accurate crystal structures for calculations. The self-consistent charge field perturbation model was also employed and was found to improve the accuracy of calculated quadrupolar coupling constants, demonstrating the impact of the neighbouring ions on the EFG tensor of the central chloride ion. Taken together, the present work contributes to an improved understanding of the factors influencing $^{35/37}$Cl NMR interaction tensors in organic hydrochlorides.

Introduction

Inorganic elements play an important role in many essential biological processes.[1] As the study of the structural and binding environments of inorganic atoms within biochemical systems continues to progress, the need for improved models and methods of study grows. Chlorine is of significant biochemical relevance as chloride ion channels are carriers of electric current across cell membranes and are consequently essential for many biological processes.[2,3] Defects in these channels result in significant health problems, such as cystic fibrosis, Bartter's syndrome, startle disease, and myotonia.[2] Knowledge of the structure of these channels has increased in recent years due in large part to the X-ray crystal structure, and subsequent studies, of the ClC ion channel.[4] We are interested in developing solid-state nuclear magnetic resonance (SSNMR) methods to examine and characterize the nature of the chloride binding environments in these and related channel systems.

X-Ray crystallography continues to provide much information on many biologically important molecules, but this technique is generally limited to materials that can be crystallized and, in some situations, is unable to probe the exact nature of the interactions between proteins and other biological molecules.[5,6] The application of NMR spectroscopy to the study of biological molecules such as proteins has proven fruitful in the determination of structure and dynamics in both the solution and solid states.[7–14] Most often, the technique is used to determine the structure of protein or nucleic acid backbones, but both solution NMR and SSNMR have also been used to directly probe the environment of inorganic metal cations in biologically relevant systems.[15–25] For example, ^{113}Cd SSNMR has been used by Ramamoorthy and co-workers to elucidate the metal cation binding environments of compounds which model metalloproteins,[23] and Lipton *et al.* have used ^{67}Zn SSNMR to characterize the zinc binding environment in zinc anhydrase.[16,17] Our own group has applied ^{23}Na SSNMR to examine the nature of noncovalent cation–π interactions in complexes which model biologically relevant systems.[24] Quantum chemical calculations often serve as an important complement to experimental SSNMR studies,

Department of Chemistry and Centre for Catalysis Research and Innovation, University of Ottawa, Ottawa, Ontario, Canada K1N6N5. E-mail: dbryce@uottawa.ca; Fax: 613-562-5170; Tel: 613-562-5800 ext. 2018

† Electronic Supplementary Information (ESI) available: Crystallographic information files (CIFs) for aspartic acid hydrochloride, cysteine hydrochloride monohydrate, and threonine hydrochloride. Difference NMR spectra for stationary samples. See DOI: 10.1039/b712688c

providing additional information to aid in the interpretation of NMR data.[17,18,20–24,26]

Both chlorine-35 (NA = 75.53%) and chlorine-37 (NA = 24.47%) are quadrupolar isotopes with nuclear spins of 3/2 and have significant quadrupole moments of −81.65 mb and −64.35 mb, respectively.[27] Until the mid-nineties, chlorine SSNMR studies had been limited by these less than favourable properties and were for the most part confined to studies of simple chloride salts.[28] With the increasing availability of high field instruments, however, studies have expanded to include a variety of more complicated inorganic and organic compounds, as well as glasses.[29] For further information, see our group's 2006 review of SSNMR of the quadrupolar halogens.[28] While the acquisition and interpretation of chlorine NMR spectra are complicated by the quadrupolar interaction, this interaction provides more information regarding the local chlorine environment. In particular, under favourable conditions, information on the electric field gradient (EFG) and chemical shift (CS) tensors can be determined. Both of these second rank tensors are highly dependent on the local molecular and electronic environments and are therefore useful in characterizing the precise local environment around an atom. In addition, the availability of high-field NMR instruments, such as the 21.1 T system at the National Ultrahigh-Field NMR Facility for Solids in Ottawa, has allowed for the study of challenging quadrupolar nuclei as, in addition to the increase in signal-to-noise ratio, the breadth of the second-order quadrupole powder pattern is inversely proportional to field strength. Provided that signal-to-noise issues can be overcome, chlorine SSNMR may be an ideal complement to X-ray diffraction in the study of small chloride ion channels, as NMR examines the local structural and electronic environment around the chloride within the channel. Chlorine SSNMR studies have previously been reported for a series of organic hydrochloride salts,[28,30–33] including recent work from our group on a series of amino acid hydrochloride salts. These studies demonstrated the utility of chlorine NMR in the characterization of chloride ion binding sites; however, study of additional model systems is still necessary in order to establish the benchmarks which will be necessary for the study of larger systems or systems of unknown structure. In addition, we are more generally interested in better understanding the fundamental relationships between the $^{35/37}$Cl EFG and CS tensors and the chloride hydrogen bonding environment in organic hydrochlorides.

In the present work, six crystalline hydrochloride salts previously uncharacterized by chlorine SSNMR, those of alanine (Ala), aspartic acid (Asp), cysteine (Cys), histidine (His), methionine (Met) and threonine (Thr), pictured in Chart 1, were studied using $^{35/37}$Cl NMR spectroscopy and complementary quantum chemical calculations. These amino acids are important residues within chloride ion channel proteins associated with disease. For example, L-alanine, L-histidine, L-threonine, L-aspartic acid and L-cysteine are all implicated in the mutations of the CLCNKB channel which lead to Bartter's syndrome type III.[34] Cysteine is also a key amino acid in the binding site of the cystic fibrosis transmembrane regulator (CFTR) ion channel, the channel associated with the devastating effects of cystic fibrosis.[35] The results presented from these six small model compounds contribute to a more general understanding of the effects of the local chlorine environment on the $^{35/37}$Cl SSNMR parameters, and further demonstrate the utility of this technique to analyze biochemically relevant chloride binding systems. In addition, quantum chemical calculations were carried out to complement the experimental data and illustrate the sensitivity of the calculated parameters to the accuracy of the structures available. The self-consistent charge field perturbation (SC-CFP) model[36] was also utilized to demonstrate the impact of surrounding ions in the crystal lattice on the chlorine SSNMR parameters.

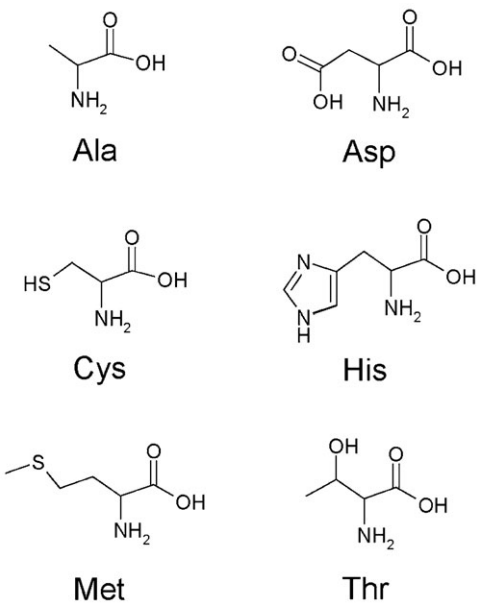

Chart 1 Structures of the amino acids whose hydrochloride salts were examined in this study.

NMR tensor conventions

Presented here are the NMR tensor conventions used in the current study. A complete description of the relevant theory of solid-state NMR spectroscopy of half-integer quadrupolar nuclei under the high-field approximation is available elsewhere.[37,38] The NMR spectra in this work were primarily affected by two interactions: the CS and quadrupolar interactions.

The nuclear magnetic shielding tensor ($\boldsymbol{\sigma}$) consists of isotropic, symmetric and antisymmetric parts. The antisymmetric component may be ignored[39] and the remaining terms may be described by a second-rank tensor which, when expressed in its principal axis system (PAS), is characterized by three eigenvalues, $\sigma_{33} \geq \sigma_{22} \geq \sigma_{11}$, and three corresponding eigenvectors. The chemical shift tensor ($\boldsymbol{\delta}$), the property measured experimentally, is also represented by three eigenvalues, $\delta_{11} \geq \delta_{22} \geq \delta_{33}$. Conversion between the magnetic shielding and chemical shift tensors is possible if an absolute shielding scale is available. For chlorine nuclei in an infinitely dilute solution of aqueous NaCl, σ_{iso}(ref) is known to be 974 ppm.[40] Therefore,

$$\delta_{iso} = 974 \text{ ppm} - \sigma_{iso} \quad (1)$$

The anisotropy and asymmetry of both the shielding and shift tensors are often described using the convenient representations of span (Ω) and skew (κ), with the isotropic parts simply equal to one-third the trace of the tensor ($\sigma_{iso} = (\sigma_{11} + \sigma_{22} + \sigma_{33})/3$; $\delta_{iso} = (\delta_{11} + \delta_{22} + \delta_{33})/3$).[41]

$$\Omega = \sigma_{33} - \sigma_{11} \approx \delta_{11} - \delta_{33} \quad (2)$$

$$\kappa = \frac{3(\sigma_{iso} - \sigma_{22})}{\Omega} \approx \frac{3(\delta_{22} - \delta_{iso})}{\Omega} \quad (3)$$

As both ^{35}Cl and ^{37}Cl have nuclear spin quantum numbers of 3/2, they will also be affected by the nuclear quadrupole interaction between the nuclear electric quadrupole moment (Q) and the EFG around the nucleus. In this work, only the chlorine-35/37 central transition (CT, $+1/2 \leftrightarrow -1/2$) was observed. All experiments assumed the high field approximation since the Larmor frequency (ν_L) was much greater than the quadrupolar frequency, $\nu_Q = 3C_Q/(2I(2I-1))$; the largest ^{35}Cl quadrupole frequency observed, 3.55 MHz, is equal to 7.2% of the Larmor frequency in the lower magnetic field (B_0 = 11.75 T; ν_L = 49.0 MHz).

The EFG tensor may be diagonalized to yield three eigenvalues in its PAS: $|V_{33}| \geq |V_{22}| \geq |V_{11}|$. These eigenvalues are often re-expressed in terms of two parameters: the quadrupolar coupling constant (C_Q) which is related to the principal component of largest magnitude, and the asymmetry parameter (η_Q).

$$C_Q = \frac{eV_{33}Q}{h} \quad (4)$$

$$\eta_Q = \frac{V_{11} - V_{22}}{V_{33}} \quad (5)$$

Along with their magnitudes, the orientations of the EFG and CS tensors relative to one another can be determined experimentally from powdered samples under favourable conditions, and are described by three Euler angles (α, β, γ). The convention used in this work is that of Arfken,[42] with the EFG PAS acting as the reference coordinate system. Using this convention, the Euler angles describe the counter-clockwise rotations of the CS tensor away from the stationary EFG reference tensor, assuming initial coincidence of the two PASs. Specifically, α describes the initial rotation about the original δ_{33} axis, β is a rotation about the new direction of δ_{22} and γ is the final rotation around the new direction of δ_{33}. Further details regarding the meaning of the Euler angles may be found in ref. 43.

Experimental and computational details

(i) Sample preparation

L-Cysteine hydrochloride monohydrate (**1**) was purchased from Aldrich and used as received. L-Alanine hydrochloride (**2**), L-aspartic acid hydrochloride (**3**), L-histidine hydrochloride monohydrate (**4**), L-methionine hydrochloride (**5**) and L-threonine hydrochloride (**6**) were prepared by dissolving the appropriate L-amino acid (Aldrich) in hot, dilute hydrochloric acid and filtering the resulting salt. Phase purity of the samples was confirmed by ^{13}C CP/MAS NMR spectra collected with a spinning rate of 4 kHz at 4.7 T and, also, by powder X-ray diffraction (*vide infra*).

Melting points were determined for all samples using a Barnstead/Electrothermal MelTemp melting point apparatus: 196–199 °C (L-alanine hydrochloride), 178–182 °C (L-aspartic acid hydrochloride), 90–93 °C (L-cysteine hydrochloride monohydrate), 237–241 °C (L-histidine hydrochloride monohydrate), 177–179 °C (L-methionine hydrochloride) and 147–150 °C (L-threonine hydrochloride).

(ii) X-Ray diffraction

All six samples were analyzed by powder X-ray diffractometry to confirm their identities. In cases where a previously published X-ray structure was available,[44–47] a theoretical X-ray powder diffraction pattern was produced using the Diamond 3.0 program.[48] In all cases, the predicted pattern and the experimental pattern were in agreement. Single crystal samples of **1**, **3**, and **6** were grown by dissolving the appropriate salt in excess dilute hydrochloric acid and allowing for slow crystallization; the structures were determined as described in the ESI.†

(iii) NMR Spectroscopy

(a) 500 MHz. Chlorine-35/37 SSNMR experiments were carried out on a 500 MHz (B_0 = 11.75 T) Bruker Avance spectrometer at the University of Ottawa. Two probes were used: a 4 mm Bruker HX probe or a 10 mm Bruker single-channel solenoid probe, tuned to 49.00 MHz (^{35}Cl) or 40.79 MHz (^{37}Cl). Samples were ground into fine powders and packed into either 4 mm o.d. zirconia rotors or 10 mm glass tubes cut to appropriate length. Experimental setup and pulse calibrations were performed using solid NaCl or NH_4Cl. All $^{35/37}$Cl NMR spectra were referenced to the $^{35/37}$Cl centreband of solid NaCl at 0 ppm and collected at room temperature. The 'solid' $\pi/2$ chlorine-35 pulse was found by halving the non-selective $\pi/2$ pulse measured on solid NaCl or NH_4Cl, and was typically 2.3 and 3.6 μs for the 4 and 10 mm probes, respectively. Typical pulse lengths for ^{37}Cl were 2.4 and 4.3 μs for the 4 and 10 mm probes, respectively. Recycle delays used were 2–5 s and signals were averaged over a period of 8–20 h. All spectra were collected under stationary conditions using the $\pi/2 - \tau - \pi/2 - \tau$-ACQ quadrupolar echo sequence. Proton decoupling was applied during acquisition on the 4 mm probe only.

(b) 900 MHz. Chlorine-35 NMR experiments were also performed on a 900 MHz (B_0 = 21.14 T) Bruker Avance II spectrometer at the National Ultrahigh-Field NMR Facility for Solids in Ottawa. A 3.2 mm Bruker DVT MAS HX probe (serial number 0001), tuned to 88.2 MHz (^{35}Cl) was used for all experiments. Experimental setup, pulse calibration and referencing were done using solid NaCl, the ^{35}Cl central-transition centreband of which was set to 0 ppm. Spectra of stationary samples were collected using the quadrupolar echo or quadrupolar Carr–Purcell–Meiboom–Gill (QCPMG) sequence.[49–52] The QCPMG experiment typically used a train of π pulses with a spacing of 200 μs following the initial $\pi/2$ pulse; this experiment was useful to rapidly assess the shape and breadth of the powder patterns. A single pulse was used

for all MAS experiments. The 'solid' $\pi/2$ chlorine-35 pulse was found to be 2.0 μs and a recycle delay of 2 s was used for all acquisitions. All experiments were done at room temperature with proton decoupling and no corrections were made for sample heating under MAS.

(iv) Data processing and simulations

All NMR spectra were processed using TopSpin 1.3. The FIDs of those experiments acquired using the quadrupole-echo pulse sequences were left-shifted as necessary. NMR spectra were simulated using the WSolids software package,[53] which incorporates the space-tiling algorithm of Alderman *et al.*[54] MAS NMR spectra were also simulated with SIMPSON,[55] using the large zcw317810 crystallite file for powder averaging in the final presented simulations.[56] Interpretations of the spectra were done within the high-field approximation and all spectra were simulated assuming a single magnetically unique site, consistent with the diffraction-based structures. Stack plots were created using DMFit.[57] Difference plots presented in the ESI† were prepared manually.

(v) Quantum chemical calculations

All quantum chemical calculations were carried out using the Gaussian 03 software package.[58] Calculations of the chlorine nuclear magnetic shielding and EFG tensors were done based on models generated using atomic coordinates from the X-ray structures of Di Blasio *et al.* for L-alanine hydrochloride[44] and L-methionine hydrochloride;[45] the atomic coordinates used for L-cysteine hydrochloride, L-aspartic acid hydrochloride and L-threonine hydrochloride were obtained from the X-ray structures collected in the present study. The atomic coordinates of the neutron diffraction structure by Fuess *et al.* were used for L-histidine hydrochloride monohydrate;[46] however, due to a typographical error in two of the coordinates,[59] the *z*-coordinate for carbon 5 and the estimated position for hydrogen 9 were taken from the X-ray structure of Donohue and Caron.[47] Using the atomic coordinates, cell parameters and space group of the amino acid hydrochloride salts, a lattice extending several unit cells in each direction was created using the Diamond program.[48] From this lattice, a chloride ion and all moieties to which it was hydrogen bonded (*i.e.*, amino acids and/or water) were selected and used as models for calculations. Prior to NMR tensor calculations, proton positions were optimized using the B3LYP method and the 3-21G* basis set, when neutron diffraction coordinates were not available for the protons.[31]

The optimal method for determining chlorine shielding and EFG tensor parameters, as determined from a previous study of similar systems,[31] was used for calculations in this study. In accordance, all EFG tensor calculations were done at the restricted Hartree–Fock (RHF) level of theory with the Dunning type cc-pVTZ basis set for the central chloride ion and the cc-pVDZ basis set was used for all other atoms. Shielding tensor calculations were done using the hybrid B3LYP DFT method using a basis set of aug-cc-pVDZ for chlorine and cc-pVDZ for all other atoms. The chlorine EFG and shielding tensors contained in the Gaussian output files were then analyzed using the EFGShield program (version 2.2).[43]

In addition, the self-consistent charge field perturbation (SC-CFP) model was employed for selected amino acid hydrochlorides. In these calculations, all chloride ions within 10.5 Å of the central chlorine were included as point charges, as described by Zhang *et al.*[36] The magnitude of the point charges was determined by matching the charge on the central chlorine to the point charges through iterative single point energy calculations. The level of theory used for the determination of the magnitude of the point charges was B3LYP/cc-pVDZ and two to five cycles were needed. The level of theory and basis sets used for the NMR tensor calculations using the SC-CFP model were the same as described above.

Results and discussion

(i) X-Ray diffractometry

In order to analyze the relationship between the local environment of the chloride ion and the chlorine NMR spectra, and to complete a full quantum chemical study of all six amino acid hydrochloride salts, atomic coordinates and unit cell parameters from X-ray or neutron diffraction studies were required. To our knowledge, no structures appear in the literature for aspartic acid hydrochloride or threonine hydrochloride. Therefore, single crystal X-ray analyses of these materials were completed. The cell parameters obtained for both salts are reported in Table 1. Threonine hydrochloride was found to crystallize in the monoclinic $P2_1$ space group while aspartic acid hydrochloride displayed triclinic $P1$ symmetry. Interestingly, these particular salts crystallize in low-symmetry space groups when compared to the structures of the salts of other L-amino acids.[44–47,60–72] The triclinic structure, indicating no symmetry, is confined to only aspartic acid hydrochloride while only four others in addition to threonine hydrochloride crystallize in the low symmetry $P2_1$ monoclinic group.[60,66,69,72] The majority of the amino acid salts crystallize in the higher symmetry orthorhombic space group.[44–47,61–63,65,71]

In addition to the two new crystal structures, an improved crystal structure for cysteine hydrochloride monohydrate was also obtained. The cell parameters are listed in Table 1. The motivation behind obtaining the improved structure was the large deviation between theoretical NMR results calculated using the published X-ray coordinates of Ayyar[61] and those

Table 1 Crystal cell parameters determined in this study for aspartic acid hydrochloride, cysteine hydrochloride monohydrate and threonine hydrochloride (see ESI for more information[fn1]†)

Aspartic acid hydrochloride	Cysteine hydrochloride monohydrate	Threonine hydrochloride
$P1$-Triclinic	$P2_12_12_1$-Orthorhombic	$P2_1$-Monoclinic
a = 5.612(2) Å α = 114.218(3)°	a = 5.4588(9) Å	a = 7.275(4) Å
b = 5.647(2) Å β = 97.874(4)°	b = 7.1570(11) Å	b = 5.263(3) Å β = 92.545(5)°
c = 6.169(2) Å γ = 95.710(4)°	c = 19.389(3) Å	c = 9.556(5) Å

determined experimentally (*vide infra*). The improved precision of the X-ray structure presented here is demonstrated by the improved *R*-value of 5.2%, compared to 12.4% for the 1968 structure. Although the two structures are quite similar, having essentially identical cell parameters, the slight improvements in atomic coordinates have a significant impact on bond distances and subsequently on the accuracy of the calculated NMR parameters (*vide infra*). The atomic coordinates for all three hydrochloride salts and details of the collection of the X-ray data may be found in the ESI.†

(ii) NMR spectroscopy

The experimentally determined quadrupolar and CS tensor data, obtained by simulation of ^{35}Cl and ^{37}Cl NMR spectra of the amino acid hydrochloride salts, are listed in Table 2. When possible, a ^{35}Cl NMR spectrum of a MAS sample was initially acquired at 21.1 T and fitted to give C_Q, η_Q, and δ_{iso}. For each of the salts, simulations were performed simultaneously on a minimum of three spectra acquired under stationary conditions: ^{35}Cl NMR spectra at both 11.75 and 21.1 T, and a ^{37}Cl NMR spectrum at 11.75 T. These simulations provided CS tensor data while the quadrupolar parameters were kept fixed. Fitting multiple spectra with the same parameters is crucial to ensure the accuracy and precision of the resulting NMR tensor parameters. Chlorine-35 QCPMG NMR spectra acquired under static conditions at 21.1 T were also collected for each salt (not shown), and these lineshapes were consistent with the corresponding powder patterns.

Examination of the data reveals the sensitivity of the EFG tensor to the local chloride ion environment, with values of $|C_Q(^{35}Cl)|$ ranging from 3.92–7.1 MHz and η_Q ranging from 0.35 to 0.94. As mentioned, the magnitude of C_Q is dependent on the largest component of the EFG tensor while η_Q is a measure of deviation of the tensor from axial symmetry. The quadrupole moment of ^{37}Cl is 78.8% that of ^{35}Cl and therefore the effect of the quadrupolar interaction decreases in chlorine-37 spectra relative to those of the chlorine-35 nucleus. To a good approximation, the remainder of the spectral parameters are identical for the two isotopes[73] and, consequently, the chlorine-37 spectrum of a material will usually be similar in appearance to the corresponding chlorine-35 spectrum except for a reduced breadth due to the decreased value of C_Q. For all of the salts in this study, the magnitude of the ^{37}Cl quadrupolar coupling constant was, within experimental error, found to be equal to 78.8% of the ^{35}Cl value, consistent with the ratio of the quadrupole moments, further confirming the accuracy and precision of the fits. Typically the magnitude of the chlorine-35 quadrupolar coupling constants measured from NMR spectra of chloride ions in organic and inorganic salts range from essentially zero to greater than 9.0 MHz,[29,74,75] and the values observed in this study cover a substantial fraction of this total range. One of the salts in the current study, aspartic acid hydrochloride, exhibited a value for C_Q larger than has previously been observed for an organic hydrochloride salt.[30,33]

The chlorine CS tensor also demonstrates sensitivity to the local chloride environment, with spans ranging from 60–100 ppm and skews ranging from −0.9 to 0.3 for the salts studied presently. These values are consistent with the range observed in previous studies of organic hydrochloride salts.

For all six samples, the anisotropic broadening of the central transition in the ^{35}Cl NMR spectrum, resulting from the second-order quadrupolar interaction and chemical shift anisotropy (CSA), was too large for the resolution of spinning sidebands from the centreband with MAS at 11.75 T, as the fastest spinning speed available was 15 kHz and the smallest spectral breadth was almost 60 kHz, for cysteine hydrochloride monohydrate. Even at the higher field of 21.1 T, the maximum spinning rate used, 22 kHz, was only sufficiently rapid for three of the salts studied: cysteine hydrochloride monohydrate, histidine hydrochloride monohydrate and methionine hydrochloride. The ^{35}Cl MAS NMR spectrum of cysteine hydrochloride monohydrate is shown in Fig. 1 along with spectral simulations performed using WSolids and Simpson. As described, the spectrum of the cysteine salt had the smallest spectral breadth observed in this study and had the quadrupolar coupling constant of smallest magnitude, 3.92 ± 0.01 MHz. The accuracy of the determined NMR parameters presented in Table 2 is clearly shown by the good agreement between the simulated and experimental spectra, with the Simpson simulation providing additional confidence in the accuracy of the determined parameters by demonstrating agreement between experimental and simulated spinning sidebands in addition to the centreband.

As mentioned, fast spinning at the magic angle averages the three principal components of the CS tensor and therefore simulations are simplified as only the isotropic shift, C_Q, and η_Q manifest themselves in the spectrum. Simulation of the spectra of stationary samples is therefore also greatly simplified as the magnitude of C_Q, the asymmetry parameter and isotropic shift are all accurately known from the MAS

Table 2 Experimental chlorine-35/37 quadrupolar and chemical shift tensor data for amino acid hydrochloride salts studied in the present work

Hydrochloride salt[a]	$C_Q(^{35}Cl)$/MHz[b]	η_Q	δ_{iso}/ppm[c]	Ω/ppm	κ	α/°	β/°	γ/°
Alanine	(−) 6.4 ± 0.1	0.75 ± 0.06	106 ± 5	60 ± 30	−0.3 ± 0.5	90 ± 15	0 ± 15	0 ± 15
Aspartic acid	(−) 7.1 ± 0.1	0.42 ± 0.05	102 ± 5	75 ± 30	−0.9 ± 0.1	0 ± 20	30 ± 20	93 ± 20
Cysteine	(−) 3.92 ± 0.01	0.47 ± 0.02	104.2 ± 0.5	66 ± 10	0.12 ± 0.12	155 ± 20	0 ± 10	0 ± 20
Histidine	(−) 4.59 ± 0.03	0.46 ± 0.02	93 ± 1	<150	[d]	[d]	[d]	[d]
Methionine	(+) 4.41 ± 0.02	0.35 ± 0.03	99 ± 1	100 ± 20	0.3 ± 0.3	93 ± 20	163 ± 15	7 ± 20
Threonine	(−) 5.4 ± 0.1	0.94 ± 0.02	99 ± 10	95 ± 40	−0.2 ± 0.5	95 ± 15	0 ± 10	0 ± 15

[a] Cysteine and histidine salts are monohydrates. [b] Chlorine-37 quadrupolar coupling constants were identical to $C_Q(^{35}Cl) \times Q(^{37}Cl)/Q(^{35}Cl) = C_Q(^{35}Cl) \times 0.788$. Negative or positive signs given in brackets are assigned based on quantum chemical calculations. [c] Isotropic chemical shifts are reported relative to solid NaCl at 0 ppm. [d] Not determined.

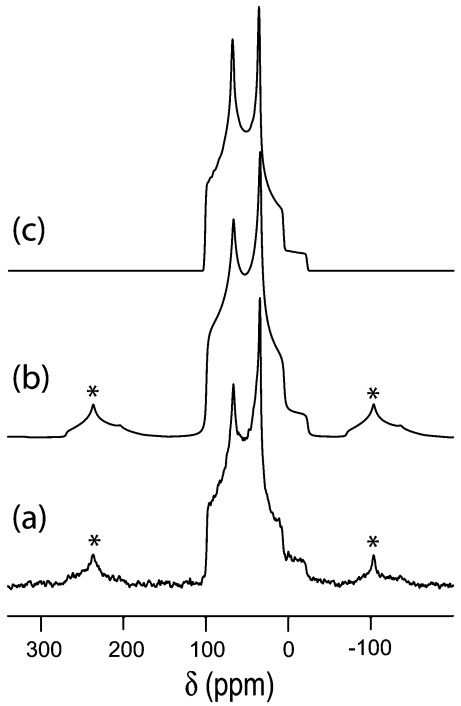

Fig. 1 Solid-state chlorine-35 MAS NMR spectroscopy of cysteine hydrochloride monohydrate at 21.1 T with ν_{rot} = 15 kHz. (a) Experimental. (b) Best fit simulation using Simpson. (c) Best-fit simulation using WSolids under the assumption of an infinite MAS rate. Spinning sidebands are indicated by asterisks.

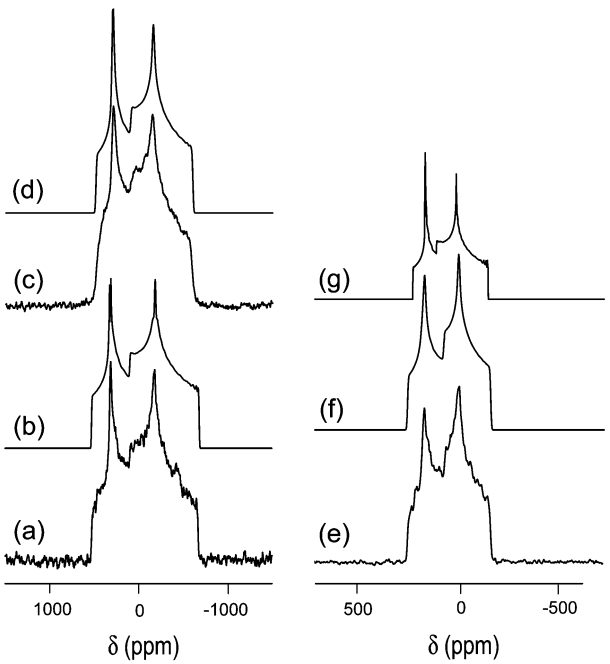

Fig. 2 Solid-state chlorine NMR spectroscopy of cysteine hydrochloride monohydrate. Experimental spectra of stationary powdered samples: (a) ^{35}Cl at 11.75 T; (c) ^{37}Cl at 11.75 T; (e) ^{35}Cl at 21.1 T. Best-fit spectra simulated with WSolids using the EFG and CS parameters listed in Table 2 appear in (b), (d) and (f). (g) Presents a simulation assuming no CSA.

spectrum. The experimental and simulated $^{35/37}$Cl NMR spectra of the cysteine salt acquired under stationary conditions are shown in Fig. 2. The small value of C_Q does not correspond to the lowest value for the CS span, consistent with the results of previous studies, although Ω is on the lower end at 66 ± 10 ppm. For all of the salts analyzed in this study, agreement between simulated and experimental spectra of stationary samples could not be achieved without the inclusion of CSA, demonstrating the importance of the chemical shift tensor interactions on the $^{35/37}$Cl lineshapes. The effects of the CS tensor on the spectral lineshapes were most apparent on the spectra of stationary powdered samples collected at 21.1 T as the effect of CSA, in hertz, is proportional to the magnetic field strength. The visibility of the CSA effect is also enhanced by the inverse relationship between field strength and the magnitude of the 2nd-order quadrupolar interaction. Based on the simulation of its ^{35}Cl MAS NMR spectrum acquired at 21.1 T (Fig. 3), methionine hydrochloride was found to have a chlorine-35 C_Q value only slightly higher than that of the cysteine salt, at 4.41 ± 0.02 MHz. Despite the similarities in the magnitude of the quadrupolar interaction for the methionine and cysteine salts, the former exhibits a larger chlorine CS span of 100 ± 20 ppm. The ^{35,37}Cl NMR spectra acquired under stationary conditions, along with simulations, appear in Fig. 4. The effect of the CS anisotropy is clearly manifested in the ^{35}Cl spectrum acquired under stationary conditions at 21.1 T, by the distinct shoulder on the low-frequency side of the spectrum. This spectral feature is visibly absent from the simulated spectrum assuming no CS anisotropy at 21.1 T included in Fig. 4.

The final salt for which a ^{35}Cl MAS spectrum could be obtained at 21.1 T was histidine hydrochloride monohydrate. The spectrum is shown in Fig. 5, along with two spectral

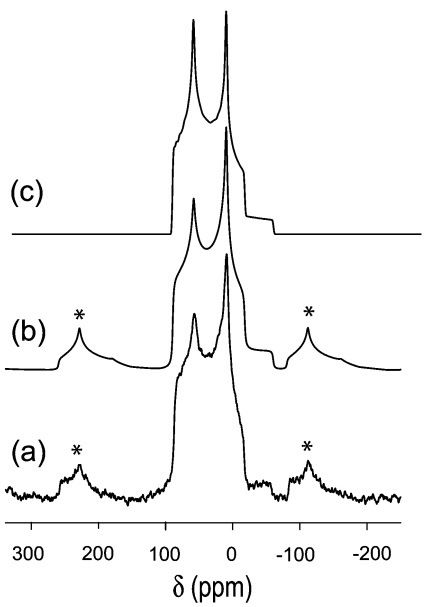

Fig. 3 Solid-state chlorine MAS NMR spectroscopy of methionine hydrochloride at 21.1 T with ν_{rot} = 15 kHz. (a) ^{35}Cl at 21.1 T and best fit simulations using (b) Simpson and (c) WSolids under the assumption of an infinite MAS rate. Spinning sidebands are indicated by asterisks.

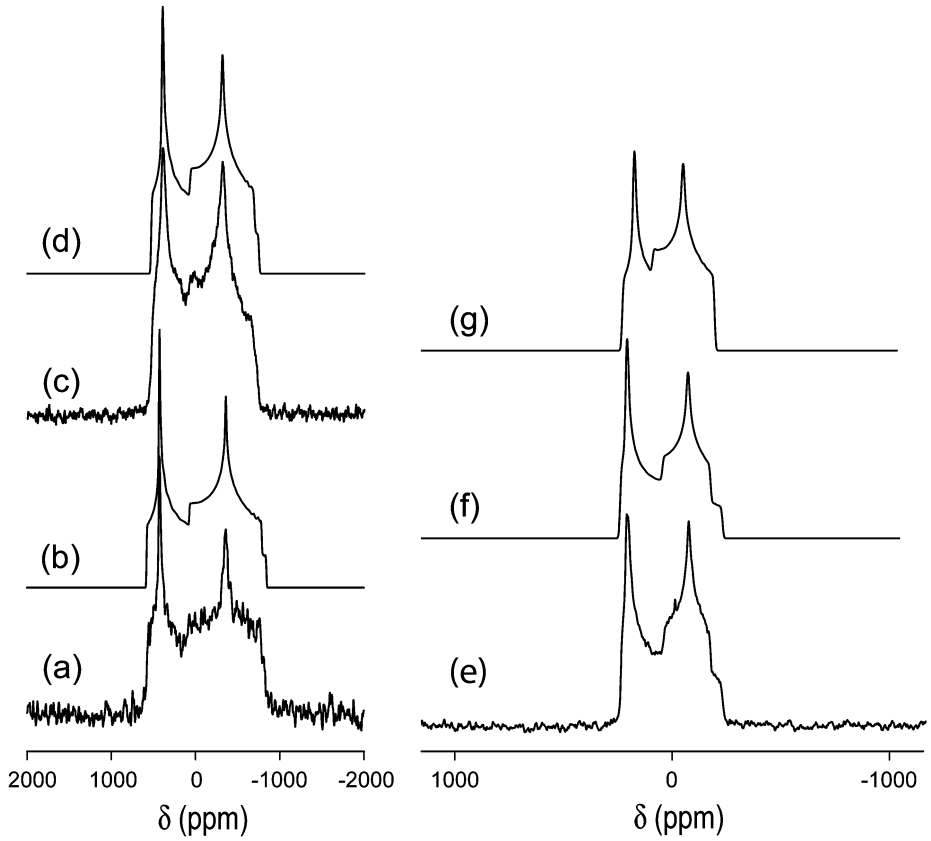

Fig. 4 Solid-state chlorine NMR spectroscopy of methionine hydrochloride. Experimental spectra of stationary powdered samples: (a) ^{35}Cl at 11.75 T; (c) ^{37}Cl at 11.75 T; (e) ^{35}Cl at 21.1 T. Best-fit spectra simulated with WSolids are shown in (b), (d) and (f). (g) Presents a simulation assuming no CSA. Trace NaCl(s) is visible in (e) at 0 ppm.

simulations. The magnitude of C_Q (^{35}Cl) was found to be 4.59 ± 0.03 MHz with an η_Q of 0.46 ± 0.02.

Shown in Fig. 6 are the ^{35}Cl NMR spectra and simulations for threonine hydrochloride collected at 11.75 and 21.1 T under static conditions. The magnitude of C_Q(^{35}Cl) was found to be intermediate amongst those in this study at 5.4 ± 0.1 MHz. The asymmetry parameter of the ^{35}Cl EFG tensor of the threonine salt is 0.94 ± 0.02, which is the closest to unity for any of the salts in the current study. This indicates that the EFG tensor deviates greatly from axial symmetry. The CS span was found to be on the higher end at 95 ± 40 ppm and thus had a significant impact on the spectral lineshape, particularly at 21.1 T, as demonstrated in Fig. 6 by the simulation assuming CS isotropy.

The ^{35}Cl NMR spectra, and spectral simulations, of alanine hydrochloride collected at the two magnetic field strengths appear in Fig. 7. The magnitude of C_Q was found to be 6.4 ± 0.1 MHz with an η_Q of 0.75 ± 0.06. Despite the large value of C_Q, the alanine salt was found to exhibit the smallest chlorine CS span of all the salts in this study at 60 ± 30 ppm. In addition, the Euler angles relating the EFG and CS tensor PASs were found to be 90, 0 and 0°, indicating that the smallest principal component of the CS tensor, δ_{33}, is coincident with the V_{33} component of the EFG tensor. Interestingly, there are no symmetry elements in the crystal structure which require this to be the case.

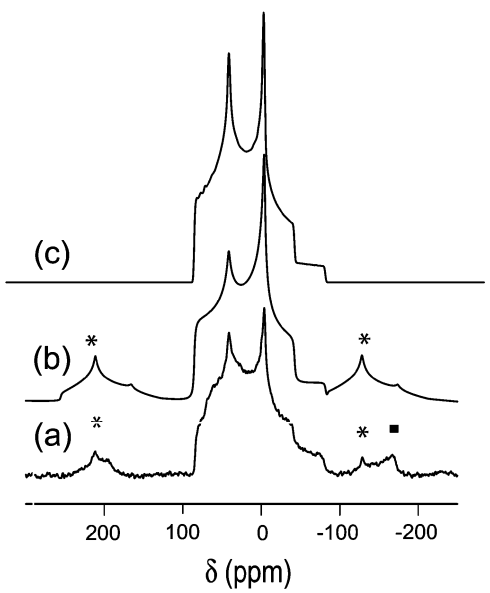

Fig. 5 Solid-state chlorine MAS NMR spectroscopy of histidine hydrochloride monohydrate at 21.1 T with ν_{rot} = 15 kHz. (a) ^{35}Cl at 21.1 T and best fit simulations using (b) Simpson and (c) WSolids assuming an infinite MAS rate. Spinning sidebands are indicated by asterisks and an impurity in the sample is indicated by a square (this prohibited a precise measurement of the chlorine CS tensor in this sample).

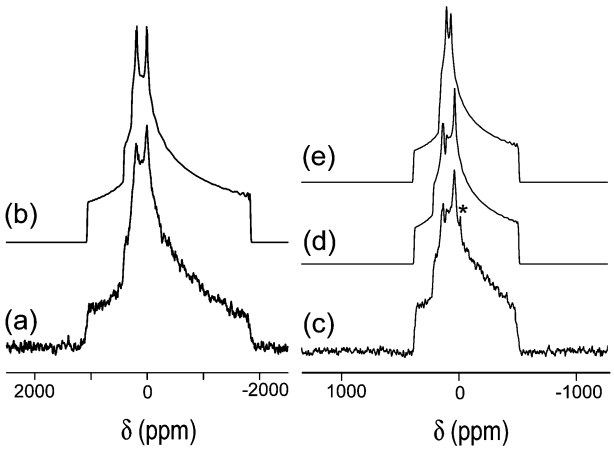

Fig. 6 Solid-state chlorine NMR spectroscopy of threonine hydrochloride. Experimental spectra of stationary powdered samples: (a) ^{35}Cl at 11.75 T and (c) ^{35}Cl at 21.1 T. Best-fit spectra simulated using WSolids appear in (b) and (d). (e) Presents a simulation assuming no CSA. The asterisk in (c) indicates trace NaCl(s).

Aspartic acid hydrochloride was found to have a C_Q of 7.1 ± 0.1 MHz, the largest observed to date for an amino acid hydrochloride, and an η_Q of 0.42 ± 0.05. The ^{35}Cl NMR spectra and accompanying simulations appear in Fig. 8. The CS tensor span was determined to be intermediate amongst those found in this study at 75 ± 30 ppm. The isotropic chemical shift of the aspartic acid salt was found to be 102 ± 5 ppm, intermediate within the study as the chlorine isotropic shifts for the six salts were all within the small range of 93–106 ppm.

(iii) Interpretation of NMR data

Using X-ray or neutron diffraction data, models of the local environment around the chloride ion in the amino acid salts were constructed in order to examine the effect of the chloride ion local environment on the ^{35,37}Cl NMR lineshapes; these models appear in Fig. 9. The models demonstrate that,

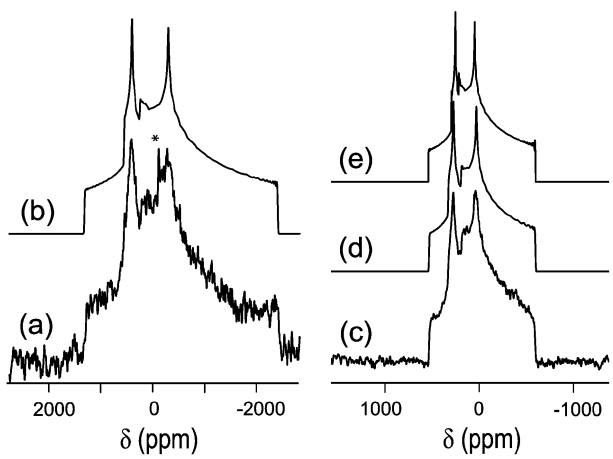

Fig. 7 Solid-state chlorine NMR spectroscopy of alanine hydrochloride. Experimental spectra of stationary powdered samples: (a) ^{35}Cl at 11.75 T and (c) ^{35}Cl at 21.1 T. Best-fit spectra simulated using WSolids appear in (b) and (d). (e) Presents a simulation assuming no CSA. The asterisk in (a) indicates trace NaCl(s).

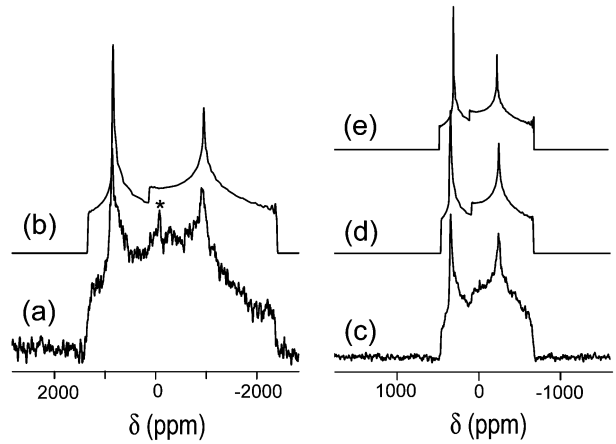

Fig. 8 Solid-state chlorine NMR spectroscopy of aspartic acid hydrochloride. Experimental spectra of stationary powdered samples: (a) ^{35}Cl at 11.75 T and (c) ^{35}Cl at 21.1 T. Best-fit spectra simulated using WSolids appear in (b) and (d). (e) Presents a simulation assuming no CSA. The asterisk indicates residual NaCl(s).

although the chloride ion in all of the salts is participating in the same type of bonding, *i.e.*, hydrogen-bonding primarily to −OH and $-NH_3$ groups (and –SH in the case of Cys $HCl \cdot H_2O$), the environments are quite different. The number of hydrogen bonds ranges from three to seven and the arrangement of the amino acids around the chloride ion varies significantly. The variation in the NMR parameters is

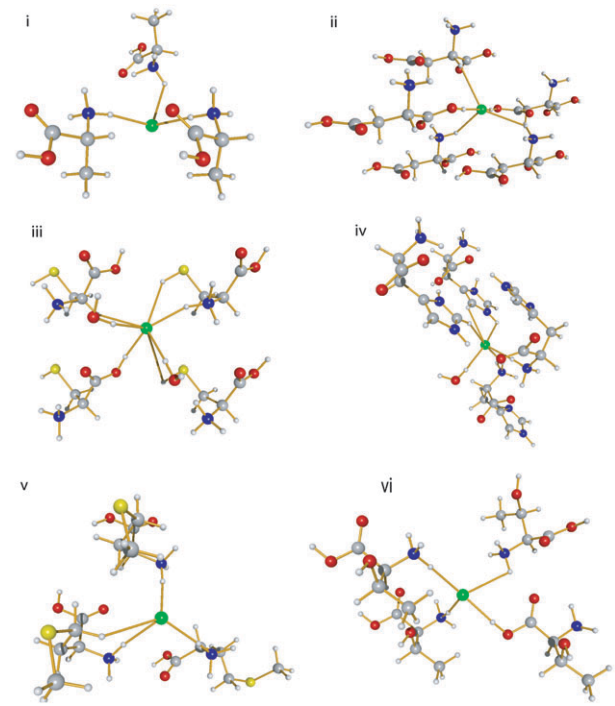

Fig. 9 Coordination environment of the chloride ion (in green) in solid (i) alanine hydrochloride, (ii) aspartic acid hydrochloride, (iii) cysteine hydrochloride monohydrate, (iv) histidine hydrochloride monohydrate, (v) methionine hydrochloride, and (vi) threonine hydrochloride. These are the models used for quantum chemical calculations of the chlorine NMR interaction tensors.

thus not surprising given the differences in the local chlorine environment.

In previous studies on organic and amino acid hydrochloride salts, two correlations were noted: firstly the magnitude of C_Q seemed to be inversely proportional to the number of hydrogen bonds at the chlorine center[33] and in addition, for amino acid hydrochloride salts, the magnitudes of C_Q and of the CS span seemed to be indirectly related to the hydrophobicity of the amino acid.[30,31] Specifically, the salts of hydrophilic amino acids were found to have small magnitudes of C_Q and Ω, while hydrophobic amino acid salts had larger values for these two parameters. These two relationships are consistent with each other, as one would expect hydrophilic amino acids to produce more hydrogen bonds in hydrochloride salts than their hydrophobic counterparts. Results from the current study also confirm that the mechanisms which control the EFG and CS tensors are quite distinct from one another, as demonstrated by the absence of correlation between the magnitudes of the CS tensor span and the quadrupolar coupling constant.

The most obvious exception to both of these previously observed trends is the salt with the largest C_Q, aspartic acid hydrochloride. Aspartic acid is a hydrophilic amino acid, and as demonstrated in Fig. 9, its HCl salt has five hydrogen bonds to the central chlorine, which is greater than the number of hydrogen bonds for the alanine, methionine and threonine salts, all of which have smaller values of C_Q. As mentioned, however, there is no symmetry in the aspartic acid hydrochloride crystal structure, unlike all other amino acid salts. This absence of symmetry is also seen in the local environment around the chlorine ion, as all the hydrogen bonds appear to be on one face of the chloride ion, while the other side is more exposed. Upon inspection, the six amino acid hydrochlorides may be divided into two separate categories on the basis of the symmetry about the chloride ion: the cysteine, methionine and histidine salts all have hydrogen bonds distributed more or less evenly about the central chloride while, like aspartic acid, the alanine and threonine salts have these bonds more heavily concentrated on one face of the ion. Previous studies have found that in ^{23}Na NMR of sodium complexes, as the symmetry of coordination about sodium deviates from perfectly symmetric (tetrahedral or octahedral), the quadrupole coupling constant increases in a consistent way: the greater the exposed area about the centre, the larger the value of C_Q.[76] For example, with deviation from octahedral symmetry, there is an increase in C_Q as the symmetry goes from octahedral, to trigonal bipyramidal to planar. The results of the current study are consistent with this model, as the three salts that have hydrogen bonds concentrated on one side of the chloride ion also have the three largest magnitudes of C_Q. In addition, the sodium studies also revealed that as symmetry deviated significantly from ideal, the quadrupole coupling constant *increased* as the number of ligands about the centre atom became larger. This relationship is consistent with the large C_Q for aspartic acid hydrochloride, indicating that when symmetry is very low about the chloride, an increase in hydrogen bonds may actually result in a larger quadrupole coupling constant, provided these additional hydrogen bonds maintain a relatively low-symmetry arrangement at Cl^-.

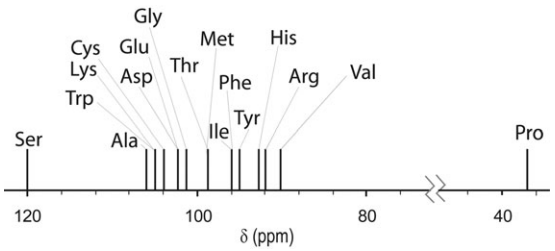

Fig. 10 Solid-state ^{35}Cl isotropic chemical shifts for seventeen amino acid hydrochlorides for which these data are available. All shifts are shown with respect to solid NaCl at 0 ppm. Data are taken from this work and from ref. 30, 31, and 33.

The ^{35}Cl isotropic chemical shifts observed in this study were between 93 and 106 ppm. These results are consistent with the results from previous studies; the majority of the chlorine isotropic chemical shifts for the seventeen amino acid hydrochlorides which have been characterized by chlorine SSNMR fall in the range of 90–110 ppm, with only serine hydrochloride and proline hydrochloride falling outside of this range.[30–33] The chlorine-35 chemical shift range for amino acid hydrochlorides is depicted in Fig. 10. The chemical shift of proline hydrochloride is the most anomalous, at 37 ppm, 53 ppm lower than the next smallest shift. The origins of the low shift of the proline salt, or the large shift of the serine salt, are not clear.

(iv) Quantum chemical calculations

The models based on the X-ray or neutron structures for the amino acid hydrochloride salts, shown in Fig. 9, were employed in quantum chemical calculations of the NMR interaction tensors. The results of these calculations are presented in Table 3. The good agreement between the experimental data and those determined through quantum chemical calculations is demonstrated in Fig. 11 and 12, which compare the experimental and best theoretical chlorine-35 quadrupolar coupling constants and CS tensor spans, respectively. With the sole exception of the aspartic acid salt, the quadrupolar coupling constants were reproduced within 12%. The aspartic acid hydrochloride calculation deviation was slightly higher, with

Table 3 Calculated chlorine-35 quadrupolar and chemical shift data for amino acid hydrochloride salts[a]

Hydrochloride salt	C_Q/MHz	η_Q	δ_{iso}[b]/ppm	Ω/ppm	κ
Alanine	−5.90	0.23	67	83	0.20
Aspartic acid	−8.33	0.19	86	111	−0.24
Cysteine	−3.48	0.43	28	72	−0.37
Cysteine[c]	−4.13	0.48	29	71	−0.52
Histidine	−4.83	0.66	103	195	−0.10
Methionine	5.00	0.15	69	90	−0.43
Threonine	−6.22	0.82	26	83	−0.45
Threonine[c]	−5.80	0.62	22	86	−0.50

[a] Quadrupolar and shielding parameters were calculated using the methods described in the Experimental. [b] To convert from calculated shielding constants to chemical shifts, a shift of 45.37 ppm was used (for the conversion from solid to aqueous NaCl chemical shift scales) in addition to the absolute shielding conversion found in eqn (1). [c] Calculated using the SC-CFP method, as described in the Experimental.

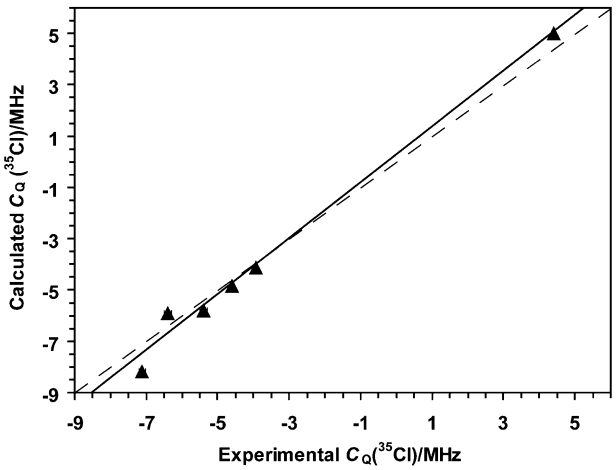

Fig. 11 Comparison between the experimentally determined chlorine-35 quadrupolar coupling constants, on the *x*-axis and the calculated values, on the *y*-axis. The calculated values plotted for the cysteine and threonine salts were determined using the SC-CFP model. The equation for the line of best fit (solid line) is $y = 1.0892x + 0.2055$, with an *R*-value of 0.994. The line $y = x$ is represented by the dashed line.

an error of 17.2%. Despite the error, it is of note that the calculation overestimates the coupling constant for the aspartic acid salt, demonstrating that its high value, compared to the other salts, is reproduced by theory. The EFG calculations also allow for designation of the sign of the quadrupole coupling constant, a classification that is not available from experiment.

Good agreement between the calculated and experimental spans was also obtained, with the calculated values all either within, or very close to within, experimental error. As was found with previous studies, however, good agreement between experimental and calculated isotropic chemical shifts was not achieved, with the calculations underestimating this parameter in all cases except for histidine hydrochloride monohydrate.

While perfect agreement between experiment and theory in all cases would be desirable, it is reassuring that, given the availability of a neutron diffraction structure, the EFG calculations for histidine hydrochloride monohydrate were most accurate. This result is in agreement with a previous study in which excellent correlation between experimental and calculated EFG tensor information was found for similar systems for which neutron diffraction structures were available.[30] However, some error is expected to be inherent in the calculations, as these were performed in the gas phase and not the solid state.

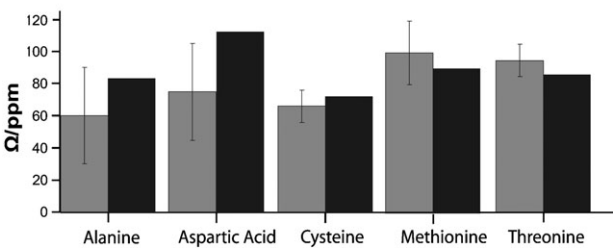

Fig. 12 Comparison between the experimentally determined CS spans (in gray) and the calculated values (in black). The calculated values plotted for the cysteine and threonine salts were determined using the SC-CFP model.

The importance of having accurate structures was also demonstrated by the improvement observed in the accuracy of the calculations of the quadrupolar and shielding parameters of cysteine hydrochloride monohydrate upon using our newly redetermined X-ray structure to construct the model; for example, the error in the calculated quadrupolar coupling constant decreases from 52 to 11% upon switching from the published structure[61] to that obtained in this study. This result highlights the utility of combining SSNMR and calculations to confirm structural characteristics.

In an attempt to improve on the calculated results for two amino acid hydrochloride salts which had large errors in C_Q (cysteine hydrochloride monohydrate and threonine hydrochloride), the SC-CFP method was also employed for the calculation of the NMR parameters. This method takes into account the effect of surrounding ionic charges in the crystal lattice in contrast to the previously discussed results which are for the isolated models shown in Fig. 9. The resulting CS spans and quadrupolar coupling constants are included in Table 3. While the SC-CFP method did slightly improve the accuracy of the span, the improvement was most significant for the magnitude of the quadrupolar coupling constant, reducing the errors in the calculation of that parameter to only 5.2 and 7.8% for the cysteine and threonine salts, respectively. The chloride–chloride internuclear distance is less than 5.1 Å in these two systems; therefore, the effect of one chloride ion on the EFG at another is not surprising. This result demonstrates that the EFG tensor at a chloride centre may be significantly affected by the surrounding chloride ions when these ions are relatively close to each other, and is not solely dependent on the local environment in the first coordination sphere, as is seen in some other systems.[77] The minimal improvement observed for the span is expected, given that the shielding tensor depends primarily on molecular orbitals with large coefficients on the central chloride; these orbitals are most strongly influenced by atoms within the first coordination sphere of the chloride ion.

Conclusions

Chlorine-35/37 SSNMR spectroscopy has been used to study the local environment of chlorine in six L-amino acid hydrochloride salts. The study has aided in the understanding of the relationship between chlorine binding environments and $^{35/37}$Cl NMR properties in organic salts. The $^{35/37}$Cl EFG and CS tensors, including their relative orientations, were determined and these demonstrated high sensitivity to slight differences in the local environment at chlorine. The accuracy of the determined parameters was ensured by the collection of data at two magnetic fields, with experiments at 21.1 T allowing for selected MAS experiments and visible manifestation of chlorine CSA in experiments run under static conditions. Chlorine-35 quadrupolar coupling constants ranged from −7.1 to 4.41 MHz with the value observed for aspartic

acid hydrochloride, −7.1 MHz, being the largest value, in magnitude, observed to date for an organic hydrochloride salt. In addition to the general trend of correlation between the hydrophobicity of the amino acid and magnitudes of C_Q and the span observed in previous studies,[30,31] symmetry about the chloride ion was demonstrated to be extremely important in determining the magnitude of C_Q, explaining the large value observed for the aspartic acid salt.

Quantum chemical calculations were found to be in good agreement with the experimental values, particularly when accurate crystal structures are available. The importance of the quality of the structure was demonstrated in the case of cysteine hydrochloride monohydrate; the calculated parameters improved significantly upon the use of the more accurate crystal structure acquired in this study. Use of the SC-CFP[36] method for calculating the NMR parameters was also found to significantly improve the accuracy of the quadrupolar coupling constants, demonstrating that the negative charges associated with neighbouring chloride ions in the structure can have a significant effect on the electric field gradient about the central nucleus, especially when the chloride–chloride internuclear distance is small.

This study, in combination with previous amino acid hydrochloride studies, has contributed some of the necessary groundwork to applying chlorine-35/37 SSNMR in the examination of the local environment of chlorine in larger systems and in systems of unknown structure.

Acknowledgements

We are grateful to Dr Glenn Facey, Dr Victor Terskikh and Dr Shane Pawsey for continued technical assistance and helpful comments. We thank Ilia Korobkov for solving the X-ray structures. D.L.B. thanks the Natural Sciences and Engineering Research Council (NSERC) of Canada for funding. Access to the 900 MHz NMR spectrometer was provided by the National Ultrahigh-Field NMR Facility for Solids (Ottawa, Canada), a national research facility funded by the Canada Foundation for Innovation, the Ontario Innovation Trust, Recherche Québec, the National Research Council of Canada, and Bruker Biospin and managed by the University of Ottawa (www.nmr900.ca). NSERC is acknowledged for a Major Resources Support grant. Some G03 calculations were carried out using the High Performance Virtual Computing Laboratory.

References

1 R. H. Holm and E. I. Solomon, *Chem. Rev.*, 1996, **96**, 2237–2238(thematic issue).
2 W. B. Guggino, in *Chloride Channels: Current Topics in Membranes*, ed. A. Kleinzeller and D. M. Fambrough, Academic Press, San Diego, 1994, vol. 42.
3 F. M. Ashcroft, *Ion Channels and Disease*, Academic Press, San Diego, 2000.
4 R. Dutzler, E. B. Campbell, M. Cadene, B. T. Chait and R. MacKinnon, *Nature*, 2002, **415**, 287–294.
5 I. L. Alberts, K. Nadassy and S. J. Wodak, *Protein Sci.*, 1998, **7**, 1700–1716.
6 A. C. Rosenzweig, D. L. Huffman, M. Y. Hou, A. K. Wernimont, R. A. Pufahl and T. V. O'Halloran, *Structure*, 1999, **7**, 605–617.
7 A. Bax, *Protein Sci.*, 2003, **12**, 1–16.
8 D. Marulanda, M. L. Tasayco, A. McDermott, M. Cataldi, V. Arriaran and T. Polenova, *J. Am. Chem. Soc.*, 2004, **126**, 16608–16620.
9 A. E. McDermott, *Curr. Opin. Struct. Biol.*, 2004, **14**, 554–561.
10 P. C. A. van der Wel, J. R. Lewandowski and R. G. Griffin, *J. Am. Chem. Soc.*, 2007, **129**, 5117–5130.
11 R. H. Havlin, F. J. Blanco and R. Tycko, *Biochemistry*, 2007, **46**, 3586–3593.
12 M. Baldus, *J. Biomol. NMR*, 2007, **39**, 73–86.
13 L. Chen, R. A. Olsen, D. W. Elliott, J. M. Boettcher, D. H. Zhou, C. M. Rienstra and L. J. Mueller, *J. Am. Chem. Soc.*, 2006, **128**, 9992–9993.
14 I. Marcotte, J. D. van Beek and B. H. Meier, *Macromolecules*, 2007, **40**, 1995–2001.
15 J. M. Aramini and H. J. Vogel, *Biochem. Cell Biol.*, 1998, **76**, 210–222.
16 A. S. Lipton, R. W. Heck and P. D. Ellis, *J. Am. Chem. Soc.*, 2004, **126**, 4735–4739.
17 A. S. Lipton, C. Bergquist, G. Parkin and P. D. Ellis, *J. Am. Chem. Soc.*, 2003, **125**, 3768–3772.
18 A. S. Lipton, T. A. Wright, M. K. Bowman, D. L. Reger and P. D. Ellis, *J. Am. Chem. Soc.*, 2002, **124**, 5850–5860.
19 A. S. Lipton, G. W. Buchko, J. A. Sears, M. A. Kennedy and P. D. Ellis, *J. Am. Chem. Soc.*, 2001, **123**, 992–993.
20 W. Huang, L. Todaro, G. P. A. Yap, R. Beer, L. C. Francesconi and T. Polenova, *J. Am. Chem. Soc.*, 2004, **126**, 11564–11573.
21 N. Pooransingh, E. Pomerantseva, M. Ebel, S. Jantzen, D. Rehder and T. Polenova, *Inorg. Chem.*, 2003, **42**, 1256–1266.
22 N. Pooransingh-Margolis, R. Renirie, Z. Hasan, R. Wever, A. J. Vega and T. Polenova, *J. Am. Chem. Soc.*, 2006, **128**, 5190–5208.
23 S. S. Kidambi, D.-K. Lee and A. Ramamoorthy, *Inorg. Chem.*, 2003, **42**, 3142–3151.
24 D. L. Bryce, S. Adiga, E. K. Elliott and G. W. Gokel, *J. Phys. Chem. A*, 2006, **110**, 13568–13577.
25 G. Wu, A. Wong, Z. Gan and J. T. Davis, *J. Am. Chem. Soc.*, 2003, **125**, 7182–7183.
26 *Calculation of NMR and EPR Parameters Theory and Applications*, ed. M. Kaupp, M. Bühl and V. G. Malkin, Wiley-VCH, Weinheim, 2004.
27 P. Pyykkö, *Mol. Phys.*, 2001, **99**, 1617–1629.
28 D. L Bryce and G. D. Sward, *Magn. Reson. Chem.*, 2006, **44**, 409–450.
29 T. O. Sandland, L.-S. Du, J. F. Stebbins and J. D. Webster, *Geochim. Cosmochim. Acta*, 2004, **68**, 5059–5069.
30 D. L. Bryce, G. D. Sward and S. Adiga, *J. Am. Chem. Soc.*, 2006, **128**, 2121–2134.
31 D. L. Bryce and G. D. Sward, *J. Phys. Chem. B*, 2006, **110**, 26461–26470.
32 C. Gervais, R. Dupree, K. J. Pike, C. Bonhomme, M. Profeta, C. J. Pickard and F. Mauri, *J. Phys. Chem. A*, 2005, **109**, 6960–6969.
33 D. L. Bryce, M. Gee and R. E. Wasylishen, *J. Phys. Chem. A*, 2001, **105**, 10413–10421.
34 D. B. Simon, R. S. Bindra, T. A. Mansfield, C. Nelson-Williams, E. Mendonca, R. Stone, S. Schurman, A. Nayir, H. Alpay, A. Bakkaloglu, J. Rodriguez-Soriano, J. M. Morales, S. A. Sanjad, C. M. Taylor, D. Pilz, A. Brem, H. Trachtman, W. Griswold, G. A. Richard, E. John and R. P. Lifton, *Nat. Genet.*, 1997, **17**, 171–178.
35 Z.-R. Zhang, G. Cui, X. Liu, B. Song, D. C. Dawson and N. A. McCarty, *J. Biol. Chem.*, 2005, **280**, 458–468.
36 Y. Zhang, S. Mukherjee and E. Oldfield, *J. Am. Chem. Soc.*, 2005, **127**, 2370–2371.
37 W. P. Power, R. E. Wasylishen, S. Mooibroek, B. A. Pettitt and W. Danchura, *J. Phys. Chem.*, 1990, **94**, 591–598.
38 S. Wi, S. E. Ashbrook, S. Wimperis and L. Frydman, *J. Chem. Phys.*, 2003, **118**, 3131–3140.
39 F. A. L. Anet and D. J. O'Leary, *Concepts Magn. Reson.*, 1991, **3**, 193–214.
40 M. Gee, R. E. Wasylishen and A. Laaksonen, *J. Phys. Chem. A*, 1999, **103**, 10805–10812.
41 J. Mason, *Solid State Nucl. Magn. Reson.*, 1993, **2**, 285–288.
42 G. B. Arfken, *Mathematical Methods for Physicists*, Academic Press, New York, 1985.
43 S. Adiga, D. Aebi and D. L. Bryce, *Can. J. Chem.*, 2007, **85**, 496–505.

44 B. Di Blasio, V. Pavone and C. Pedone, *Cryst. Struct. Commun.*, 1977, **6**, 745–748.
45 B. Di Blasio, V. Pavone and C. Pedone, *Cryst. Struct. Commun.*, 1977, **6**, 845–848.
46 H. Fuess, D. Hohlwein and S. A. Mason, *Acta Crystallogr., Sect. B: Struct. Crystallogr. Cryst. Chem.*, 1977, **33**, 654–659.
47 J. Donohue and A. Caron, *Acta Crystalogr.*, 1964, **17**, 1178–1180.
48 K. Brandenburg, *Diamond*, version 3.0e, Crystal Impact GbR, Bonn,Germany, 1997–2005.
49 H. Y. Carr and E. M. Purcell, *Phys. Rev.*, 1954, **94**, 630–638.
50 S. Meiboom and D. Gill, *Rev. Sci. Instrum.*, 1958, **29**, 688–691.
51 J. T. Cheng and P. D. Ellis, *J. Phys. Chem.*, 1989, **93**, 2549–2555.
52 F. H. Larsen, H. J. Jakobsen, P. D. Ellis and N. C. Nielsen, *J. Phys. Chem. A*, 1997, **101**, 8597–8606.
53 K. Eichele and R. E. Wasylishen, *WSOLIDS NMR Simulation Package version 1.17.30*, Universität Tübingen, Tübingen, Baden-Württemberg, Germany, 2001.
54 D. W. Alderman, M. S. Solum and D. M. Grant, *J. Chem. Phys.*, 1986, **84**, 3717–3725.
55 M. Bak, J. T. Rasmussen and N. C. Nielsen, *J. Magn. Reson.*, 2000, **147**, 296–330.
56 Downloaded from http://bionmr.chem.au.dk/download/simpson/crystal_files/ accessed November 2007.
57 D. Massiot, F. Fayon, M. Capron, I. King, S. Le Calvé, B. Alonso, J.-O. Durand, B. Bujoli, Z. Gan and G. Hoatson, *Magn. Reson. Chem.*, 2002, **40**, 70–76.
58 M. J. Frisch, G. W. Trucks, H. B. Schlegel, G. E. Scuseria, M. A. Robb, J. R. Cheeseman, J. A. Montgomery, Jr, T. Vreven, K. N. Kudin, J. C. Burant, J. M. Millam, S. S. Iyengar, J. Tomasi, V. Barone, B. Mennucci, M. Cossi, G. Scalmani, N. Rega, G. A. Petersson, H. Nakatsuji, M. Hada, M. Ehara, K. Toyota, R. Fukuda, J. Hasegawa, M. Ishida, T. Nakajima, Y. Honda, O. Kitao, H. Nakai, M. Klene, X. Li, J. E. Knox, H. P. Hratchian, J. B. Cross, C. Adamo, J. Jaramillo, R. Gomperts, R. E. Stratmann, O. Yazyev, A. J. Austin, R. Cammi, C. Pomelli, J. W. Ochterski, P. Y. Ayala, K. Morokuma, G. A. Voth, P. Salvador, J. J. Dannenberg, V. G. Zakrzewski, S. Dapprich, A. D. Daniels, M. C. Strain, O. Farkas, D. K. Malick, A. D. Rabuck, K. Raghavachari, J. B. Foresman, J. V. Ortiz, Q. Cui, A. G. Baboul, S. Clifford, J. Cioslowski, B. B. Stefanov, G. Liu, A. Liashenko, P. Piskorz, I. Komaromi, R. L. Martin, D. J. Fox, T. Keith, M. A. Al-Laham, C. Y. Peng, A. Nanayakkara, M. Challacombe, P. M. W. Gill, B. Johnson, W. Chen, M. W. Wong, C. Gonzalez and J. A. Pople, *GAUSSIAN 03, (Revision C. 02)*, Gaussian, Inc., Wallingford, CT, 2004.
59 X. Zhao and G. S. Harbison, *J. Phys. Chem. B*, 2006, **110**, 25059–25065.
60 J. Dow, L. H. Jensen, S. K. Mazumdar, R. Srinivasan and G. N. Ramachandran, *Acta Crystallogr., Sect. B: Struct. Crystallogr. Cryst. Chem.*, 1970, **26**, 1662–1671.
61 R. R. Ayyar, *Z. Kristallogr. Bd.*, 1968, **126**, 227–239.
62 A. Sequeira, H. Rajagopal and R. Chidambaram, *Acta Crystallogr., Sect. B: Struct. Crystallogr. Cryst. Chem.*, 1972, **28**, 2514–2519.
63 N. Shamala and K. Venkatesan, *Cryst. Struct. Commun.*, 1972, **1**, 227–229.
64 A. R. Al-Karaghouli, F. E. Cole, M. S. Lehmann, C. F. Miskell, J. J. Verbist and T. F. Koetzle, *J. Chem. Phys.*, 1975, **63**, 1360–1366.
65 K. I. Varughese and R. Srinivasan, *Pramana*, 1976, **6**, 189–195.
66 L. Golič and W. C. Hamilton, *Acta Crystallogr., Sect. B: Struct. Crystallogr. Cryst. Chem.*, 1972, **28**, 1265–1271.
67 R. R. Bugayong, A. Sequeira and R. Chidambaram, *Acta Crystallogr., Sect. B: Struct. Crystallogr. Cryst. Chem.*, 1972, **28**, 3214–3219.
68 A. R. Al-Karaghouli and T. F. Koetzle, *Acta Crystallogr., Sect. A: Cryst. Phys., Diffr., Theor. Gen. Crystallogr.*, 1975, **B31**, 2461–2465.
69 T. J. Kistenmacher, G. A. Rand and R. E. Marsh, *Acta Crystallogr., Sect. B: Struct. Crystallogr. Cryst. Chem.*, 1974, **30**, 2573–2578.
70 T. Takigawa, T. Ashida, Y. Sasada and M. Kakudo, *Bull. Chem. Soc. Jpn.*, 1966, **39**, 2369–2378.
71 M. N. Frey, T. F. Koetzle, M. S. Lehmann and W. C. Hamilton, *J. Chem. Phys.*, 1973, **58**, 2547–2556.
72 T. F. Koetzle, L. Golic, M. S. Lehmann, J. J. Verbist and W. C. Hamilton, *J. Chem. Phys.*, 1974, **60**, 4690–4696.
73 C. J. Jameson, in *Encyclopedia of NMR*, ed. D. M. Grant and R. K. Harris, John Wiley, New York, 1996, pp. 2638–2655.
74 S. Hayashi and K. Hayamizu, *Bull. Chem. Soc. Jpn.*, 1990, **63**, 913–919.
75 T. L. Weeding and W. S. Veeman, *J. Chem. Soc., Chem. Commun.*, 1989, 946–948.
76 H. Koller, G. Engelhardt, A. P. M. Kentgens and J. Sauer, *J. Phys. Chem.*, 1994, **98**, 1544–1551.
77 H. Koller, E. L. Meijer and R. A. van Santen, *Solid State Nucl. Magn. Reson.*, 1997, **9**, 165–175.

